JOURNAL OF CATALYSIS 127, 213–220 (1991)

EXAFS Evidence of Carbon Monoxide-Induced Growth of Pd Particles Encaged in Zeolite Y

ZONGCHAO ZHANG, HUAIYU CHEN,[1] LIEN-LUNG SHEU, AND WOLFGANG M. H. SACHTLER

Ipatieff Laboratory, Center for Catalysis and Surface Science, Northwestern University, Evanston, Illinois 60208

Received February 26, 1990; revised June 4, 1990

EXAFS data of Pd in zeolite NaY show that after calcination at 500°C and reduction at 350°C small Pd clusters are formed in the supercages of the zeolite with a compressed Pd–Pd distance of 2.68 Å and an average coordination number of CN = 4, corresponding to nuclearity of 6 Pd atoms. Adsorption of CO results in a significantly increased cluster size and a relaxed Pd–Pd distance of 2.70 Å. The average coordination number of Pd (CN = 6) is consistent with Pd clusters of 13 atoms which are confined in the supercages by the dimension of the windows. The enhanced rate of coalescence due to CO indicates that CO adsorption weakens not only Pd–Pd bonds in the cluster, but also the interaction of the cluster with the zeolite. However, no Pd cluster disintegration by CO adsorption is observed.

I. INTRODUCTION

Carbonyl clusters are known for most platinum group metals (*1*), e.g., $Ru(CO)_5$, $Ru_2(CO)_9$, $Ru_3(CO)_{12}$, $Os_7(CO)_{21}$, $Rh_4(CO)_{12}$, $Rh_6(CO)_{16}$, and similar clusters of Ir. However, carbonyl clusters of Pd and Pt have been reported only in noble gas matrices below 20 K (*2*), in molecular beams of He where Pd_nCO and $Pd_n(CO)_2$ were detected (*3*); or, very recently, in zeolite cages (*4–6*). These observations suggest that Pd and Pt carbonyls can only exist in an inert environment where the carbonyl clusters are isolated from each other.

The chemistry of $Pd_n(CO)_x(PR_3)_y$, where R represents an alkyl group such as Et, Me, or Bu, is better known. In organic media under inert atmosphere, these polynuclear carbonylphosphine clusters are stable in the presence of phosphine ligands (*7, 8*). The nuclearity **n** of the clusters varies with the concentration of phosphine ligands. Upon removing phosphine, transformation from $n = 4$ to $n = 10$ is observed (*9*). Further abstraction of phosphine leads to even higher nuclearity, e.g., $n = 23$ and $n = 38$ (*10, 11*). This increase of cluster nuclearity with decreasing phosphine concentration suggests coalescence of an unstable $Pd_n(CO)_x$ species in organic solutions.

The structure of zeolites, particularly those of faujasite type with well-defined cages, favors isolation of metal carbonyl complexes from each other (*12, 13*). Previously, we reported that rhenium hydridocarbonyls, which are very unstable in solution, are (meta-) stable in faujasite cages because they cannot react with each other (*13*). Our recent findings that carbonyl clusters of Pd (*4–6*) and Pt (*14*) can form in the supercages of NaY zeolite, suggest that isolation of the encaged species is essential for their (meta-) stability. It has been reported that $Pd_n(CO)_x$ with $n = 13$ would fit perfectly into a faujasite supercage, but it should also be noted that clusters with much lower nuclearity will be unable to pass through the 7.5 Å cage aperture and, there-

[1] Physics Department, Illinois Institute of Technology, Chicago, IL 60616, USA.

0021-9517/91 $3.00

fore, remain encaged in these zeolite cages. A lower nuclearity is indeed suggested by analogy with zeolite-encaged rhodium carbonyl clusters, for which extensive documentation exists (*15–18*) Tetra- and hexanuclear clusters $Rh_4(CO)_{12}$ and $Rh_6(CO)_{16}$ are formed by treatment of Rh precursors with a mixture of CO and H_2O (*15, 19*). However, the analogy of Rh and Pd clusters is limited; unlike $Pd_n(CO)_x$ which releases CO at room temperature (*4*), the $Rh_6(CO)_{16}$ clusters encaged in the same zeolite do not release any observable CO upon purging with Ar (*20*). Additionally, no ^{13}CO isotope exchange takes place below 340 K (*15*). Because the reduction of the Rh^{3+} cation generates protons which display high Brønsted acidity, neutralization of the zeolite support during reduction has a marked effect on the identity of the carbonyl species formed. Very recently, IR bands were discovered in our laboratory due to a new Rh carbonyl species, possibly $Rh_2(CO)_8$ with no bridging CO, formed by reduction of Rh^+ in the presence of NH_3 (*20*). Van't Blik *et al.* (*21*) and Bergeret *et al.* (*22*) have reported that Rh particles, supported on Al_2O_3 or zeolite Y, disintegrate upon CO admission to form stable $RH^+(CO)_2$. The authors attribute the disintegration to the superior strength of the Rh–CO bond, in comparison to Rh–Rh (*23*).

Summarizing the available evidence, it can be inferred that palladium carbonyl clusters encaged in supercages of NaY exist, but their nuclearity is at present unknown. Conclusions based solely on analogy with rhodium carbonyl clusters are not reliable because the Pd–CO bond strength is apparently weaker than the Rh–CO bond strength. It is further unknown whether bare Pd_n particles in NaY have the same nuclearity prior to admission of CO as the $Pd_n(CO)_x$ clusters responsible for the characteristic FTIR spectra reported previously. It cannot be ruled out, at present, that CO admission might either disintegrate larger Pd_n clusters or, conversely, that highly mobile and unstable carbonyl intermediates of low nuclearity promote Ostwald ripening, i.e., increase the size of more stable Pd_n nuclei at the expense of less stable ones. EXAFS results of Möller and Bein show that bare Pd clusters of low nuclearity can be prepared in NaY by reduction at low temperature (*24, 25*); the genesis of highly dispersed Pd in-NaY has been studied in fair detail by TPO, TPR, and TPD techniques (*26, 27*). The goal of the present study is twofold: (1) establish the nuclearity of Pd clusters after admission of CO in NaY supercages and (2) compare it with the nuclearity of the bare Pd particles prior to admission of CO.

II. EXPERIMENTAL

a. Sample Preparation

Three 5 wt% Pd/NaY samples were studied with EXAFS spectroscopy. Ion exchange was carried out by adding $Pd(NH_3)_4(NO_3)_2$ solution (0.01 *M*) dropwise to a slurry of NaY (LZY-52, Union Carbide) at 20°C. The slurry was stirred for an additional 24 h. After filtration, the sample was washed with deionized water to remove NO_3^- ions. Each sample was calcined from 20 to 500°C at 0.5°C/min in a flow of O_2 (2000 ml/min per gram of sample) and maintained at 500°C for 2 h. Under these calcination conditions, ammine ligands are oxidized to completion and all water molecules are removed. The sample was subsequently purged with Ar at 500°C for 20 min prior to cooling down to 20°C for reduction. For simplicity, each sample will be referred to as T_2/t, i.e., reduction at T_2 (°C) for t min. Reduction was performed in an H_2 stream by increasing the temperature from 20°C to T_2 at 8°C/min. The samples were purged with Ar for an additional 20 min at T_2 after reduction. T_2/t/CO refers to further treatment with CO after $T2/t$. The sample 500/480 was prepared individually. The sample 350/20/CO was prepared from the same batch as 350/20. After loading 350/20 (half of the batch) to a sample holder in a drybox, the remainder of the sample was sealed in the reactor with teflon stopcocks. The sample was then placed in a flowing stream of CO for 10 min at room temperature. This

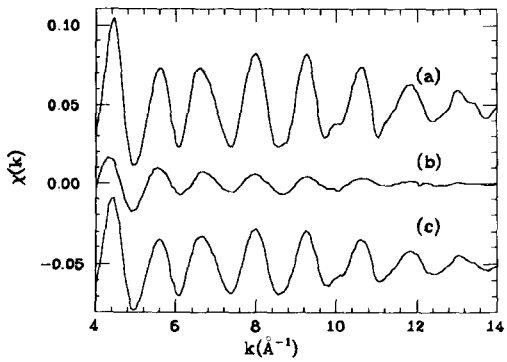

FIG. 1. Normalized EXAFS $\chi(k)$ functions of reduced Pd/NaY samples; (a) T_2 = 500°C, t = 480 min; (b) T_2 = 350°C, t = 20 min; (c) same as (b) after admission of CO at room temperature and He purging at room temperature for 20 min.

sample was then purged with He at 21°C for 20 min and is referred to as 350/20/CO. As mentioned above, each sample was sealed in a quartz reactor after the gas treatment. Samples were pressed into pellets (400 mg for each sample) in a drybox under circulating N_2 atmosphere and placed into individual aluminum sample holders. These holders were sealed with Kapton film. Each sample holder was stored in a vial sealed with parafilm. The vials were further sealed in a N_2 environment in jars with parafilm before transportation to the synchrotron.

b. EXAFS Data Collection

EXAFS data, following the Pd K-edge at 24350 eV, were collected at X18b of NSLS at Brookhaven National Laboratory. The ring energy is at 2.5 GeV. Typical filled current is 200 mA. The monochromator Si(111) crystal was detuned by 30% during data collection. A stainless-steel cell, especially designed for transmission EXAFS measurements at liquid nitrogen temperature, is used. Aluminum sample holders are attached to a die which fits perfectly in the center of a cylindrical cavity. Directly above the cavity is a stainless-steel liquid nitrogen dewar with a vacuum jacket for insulation. Liquid nitrogen temperature was maintained throughout the data collection. Both ends of the cavity are sealed by stainless-steel flanges with copper gaskets. The window of each flange is epoxy sealed with Kapton film. During data collection, cold nitrogen gas flows through the cavity to maintain an inert atmosphere. Water circulates continuously through the jackets at both ends of the cavity to prevent condensation of moisture on the Kapton window.

Data analysis was performed with the University of Washington software package. The k range from 4 to 14 in χ data is used for Fourier transform. The R window used for inverse transform is from 2.0 to 3.0. A 0.025-mm Pd foil and PdO powder were used as reference structures for the EXAFS data analysis. The coordination number (CN) of Pd in the reference foil is taken as 12, and the Pd–Pd bond distance (R) in the foil is assigned to 2.75 Å. In the PdO power reference, CN = 4 and R, the distance of Pd–O, is 2.01 Å.

III. RESULTS

The normalized EXAFS $\chi(k)$ functions are shown in Fig. 1. Traces a, b, and c correspond to 500/480, 350/20, and 350/20/CO, respectively. Sample 350/20 shows the lowest amplitude of the three. The k^2-weighted Fourier transforms of the EXAFS signals in R-space are shown in Fig. 2. Trace a corre-

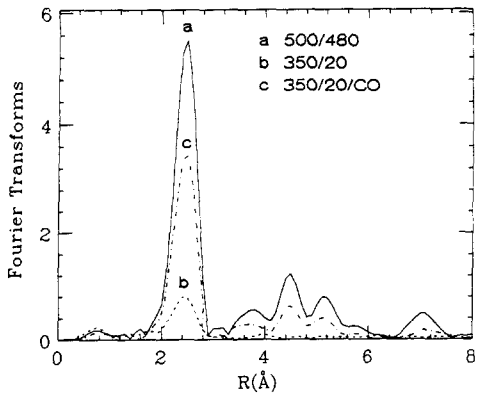

FIG. 2. k^2-weighted Fourier transforms of EXAFS function of reduced Pd–NaY samples: (a) T_2 = 500°C, t = 480 min; (b) T_2 = 350°C, t = 20 min; (c) same as (b) after admission of CO at room temperature and He purging at room temperature for 20 min.

sponds to sample 500/480; trace b 350/20; and trace c 350/20/CO. The main peak in each trace represents the Pd–Pd contribution. Trace a has the highest amplitude. Compared to trace c, trace b has a significantly smaller amplitude. Qualitatively, this means that the Pd atoms in sample 350/20 have, on average, fewer coordinating Pd neighbors than the Pd atoms in sample 350/20/CO.

The contribution from first nearest neighboring Pd atoms, shown in Fig. 3, is obtained by reverse Fourier-filtered transform of the main peak for each corresponding trace in Fig. 2. Visual comparison reveals again that the amplitude is highest for sample 500/480, and much smaller for sample 350/20, particularly in comparison to that of sample 350/20/CO.

These data were fitted with a combination of a Pd–Pd shell (Pd foil reference) and a Pd–O shell (PdO powder reference) using EXCURVE (*28*). Satisfactory fits were obtained for samples 500/480 and 350/20/CO, without including the Pd–O shell. However, it was necessary to use a two-shell fit for sample 350/20. These curve fits are shown in Fig. 2. The optimized parameters obtained from the fittings are listed in Table 1. Sample 500/480 has a Pd–Pd bond distance of 2.71 Å and coordination number of 7.8. Sample 350/20 has a slightly shorter Pd–Pd distance (R_{Pd-Pd} = 2.68 Å) and smaller CN of 4.0. The sample 350/20/CO, i.e., after admission of CO to the same batch of 350/20 at 21°C and purged with He at the same temperature for 20 min, however, retains a CN of 6.0 and R_{Pd-Pd} of 2.70 Å.

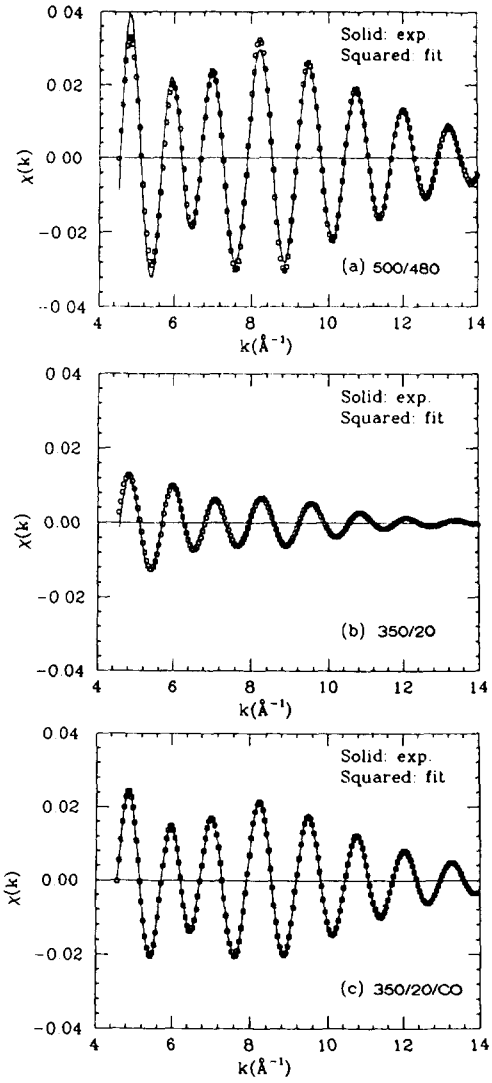

FIG. 3. Curve fittings to the inverse Fourier transforms of the first peak of the radial distribution functions as shown Fig. 2.

IV. DISCUSSION

From the EXAFS results it is obvious that the sample which was reduced at 500°C for 8 h contains large Pd particles compatible with the dimensions of the supercages. The coordination number of 7.8 is consistent with the 41-atom cluster of Pd which completely fills the supercage. Pd–Pd bond distances from second nearest neighbors to further neighbors extending to 7 Å are observed in Fig. 2. This is expected, as previous X-ray studies by Gallezot *et al.* (*29–31*) showed the formation of large Pd particles by reduction of Pd/NaY at such high temperatures.

Previous temperature-programmed reduction and desorption studies (*26, 27*), as well as X-ray diffraction studies (*29, 31*), showed that the dispersion of Pd in NaY is strictly determined by the pretreatment conditions. After calcination at 500°C, Pd^{2+}

TABLE 1

EXAFS Parameters for PdNaY after Different Treatments

Sample	Pd–Pd			Pd–O		
	N	R	$\Delta\sigma^2 \times 100$	N	R	$\Delta\sigma^2 \times 100$
500/480	7.8	2.71	0.47			
350/20	4.0	2.68	1.5	1.2	2.17	1.1
350/20/CO	6.0	2.70	0.61			

Note. N, average coordination number (±10%). R, interatomic distance (± 0.01 Å). $\Delta\sigma^2$, thermal and static disorder relative to reference compound.

ions are located in sodalite cages. Subsequent reduction at low temperature (e.g., 200°C) leads to atomically dispersed Pd in sodalite cages. These Pd atoms are unable to dissociatively adsorb H_2; therefore a low H/Pd ratio is observed. With increasing reduction temperature, these atoms move into supercages, where they agglomerate to particles capable of adsorbing hydrogen; the H/Pd ratio thus passes through a maximum at a reduction temperature of 350°C. A similar dependence on the reduction temperature is observed for the FTIR intensity of adsorbed CO in the bridging mode (*5*). Therefore, it can safely be assumed that in sample 350/20 the overwhelming majority of the Pd particles will be located in supercages.

The most striking result of the present study is the change of Pd particle size induced by CO, as demonstrated by the EXAFS spectra of samples 350/20 and 350/20/CO. For example, 350/20, the coordination number of 4.0, suggests an average particle of 6 atoms such as a regular octahedron, and concomitantly, there is a significant Pd–Pd bond contraction (2.68 Å for 350/20 vs 2.75 Å for bulk Pd). Additionally, the Pd particles in this sample are highly disordered, as indicated by the value of $\Delta\sigma^2$. On the other hand, the particle size in the 350/20/CO sample shows a substantial increase with respect to 350/20. With allowances for experimental error (±20%), this coordination number of 6.0 is consistent with a 13-atom particle, which could be either a cubooctohedron (CN = [12 × 5 + 1 = 12]/13 = 5.5) or an icosahedron (CN = [12 × 6 + 1 × 12]/13 = 6.5). In addition, the Pd–Pd bond length is found relaxed from 2.68 Å in sample 350/20 to 2.70 Å in sample 350/20/CO. Corresponding to the increase of particle size, disorder is much lower (2.5 times) in sample 350/20/CO than in sample 350/20, as follows from the value of $\Delta\sigma^2$.

Our previous FTIR study showed that adsorbed CO on Pd clusters can be partially purged off at room temperature by inert gas such as Ar (*4*). In the present investigation, He gas was used to purge CO at 21°C for 20 min at the end in the preparation of 350/20/CO. The sample was further exposed to circulating N_2 gas in drybox in the process of making a pellet. Even though CO may be partially retained in the sample 350/20/CO, it is not reliable to obtain the number of CO in this *ex situ* experiment. In addition, due to the much stronger back-scattering potential of Pd in comparison to C or O and the high coordination of Pd–Pd for 350/20/CO, the inverse Fourier transform of the first peak can be fitted reasonably well by one term without including C and O. However, for sample 350/20, the coordination due to Pd in the first shell is so low that the contribution of O to the EXAFS becomes important. Based on our previous TPD results, the coordinating O atoms, which contributed to the first peak, originate from the interaction of small Pd primary particles with supercage walls, rather than from an interaction of iso-

lated Pd atoms with the walls (*26, 27*). Isolated Pd atoms in sodalite cages prevail only at low reduction temperatures, e.g., 200°C. The interatomic distance contraction for sample 350/20 is in accordance with results on other extremely small and isolated metal clusters (*32, 33*). EXAFS data of Ni and Cu metal clusters on amorphous carbon substrates, prepared by vapor deposition, demonstrate that the interatomic metal–metal distances in the cluster contract with decreasing particle size (*34*). A recent EXAFS study by Yokoyama *et al.* also showed substantially shorter Pd–Pd bond distances (2.69 Å) for small Pd clusters on silica support than for the bulk metal (*35*). This phenomenon is rationalized assuming a more free-atom-like configuration of the metal atoms as the cluster size decreases (*36, 34*).

The fact that after CO adsorption the nuclearity of Pd_n clusters is found increased shows that the prevailing phenomenon is not disintegration of bare Pd clusters, but an enhanced coalescence. Potential causes of this phenomenon must be discussed: Prior to CO adsorption, the small Pd clusters are probably stabilized by interaction with zeolite walls. They also share the zeolite cages with Na^+ and H^+ ions; interaction of Pd with these ions is conceivable. The analogous system of Ir_4 clusters with Mg^{2+} ions has been theoretically analyzed by van Santen (*37*). As a result of these interactions, Pd clusters are expected to be polarized. In fact, electron deficient Pd metal particles, even partially approaching Pd^+, have been reported on zeolite supports (*38, 39*). Evidence for the interaction of protons, both with bare Pd clusters and with Pd carbonyl clusters, has been obtained recently (*6*). The $Pd_nH_x^+$ adducts manifest themselves as electron-deficient Pd particles of high catalytic activity (*40*); an interaction of Pd with charge-compensating zeolite ions has been suggested by recent FTIR results of CO adsorbed on Pd particles in CaNaY and Mg NaY, both with free zeolite protons and after their neutralization with NH_3 (*41*). An effect of cations on the catalytic activity of supported Pd particles has also been reported to be essential in methanol synthesis (*42*).

It appears that adsorption of CO on Pd_n clusters not only weakens metal–metal bonds, resulting in a relaxation of the Pd–Pd distance, but it also lowers the extent of interaction between cluster and zeolite walls, protons, and Na^+ ions. Concomitantly, carbonyl clusters are formed which initially will have the same nuclearity as the bare cluster. But the activation energy for cluster migration through supercage channels will be lower for small carbonyl clusters than for bare Pd clusters. The primary carbonyl clusters are unstable, as follows from the evidence with clusters in organic solution; they tend to coalesce with each other. Because the actual cluster sizes after metal reduction are distributed around the average value, the smaller particles will easily pass through the cage windows of 7.5 Å. Migration and coalescence will cease once the clusters have reached a critical size, preventing their migration through cage apertures. With this migration and growth mechanism, it is conceivable that some Pd clusters consist of more than 13 atoms, as primary Pd carbonyl clusters will also migrate to the larger immobilized Pd clusters. It is therefore not surprising that remote Pd shells at distances as far as 7 Å from absorbing Pd atoms for 350/20/CO become visible in Fig. 2. As pointed out prevously, CN = 5.5 and CN = 6.5 correspond to the cuboctohedron and icosahedron, respectively. A coordination number of 6 from our fit of the first Pd–Pd shell still suggests to us that Pd_{13} clusters prevail in sample 350/20/CO. Previously, we showed that a Pd carbonyl cluster with 13 Pd atoms will completely fill a zeolite supercage with the linear CO ligands actually pointing through cage windows (*4*). The Pd–Pd bond length slightly increases from 350/20 to 350/20/CO, although this increase remains within experimental error. Nevertheless, it seems logical that, as a result of the coalescence, Pd–Pd bonds are relaxed. Their length increases from 2.68 to 2.70 Å. The large Pd clusters after the admission of CO are more ordered than the

primary Pd metallic clusters before the introduction of CO.

While no reason exists to exclude Ostwald ripening as another cause contributing to the growth of particles, there is no evidence for any disintegration of Pd clusters as a consequence of CO adsorption. In this respect Pd clusters appear to be different from Rh clusters. This is in accordance with the different chemical natures of Pd and Rh. $Rh^+(CO)_2$ is a thermodynamically stable species, especially in proton-rich environment, but Pd carbonyls of low nuclearity appear to be unstable (*43, 8*); they have been detected only in systems where they were isolated one from another (*2, 4–6*).

Pd clusters even smaller than those in the present study were reported in another EXAFS study, where much lower reduction temperatures were used (*44, 45*). Under those conditions, even Pd trimers were observed, but no contraction of the Pd–Pd. Presumably, adsorbed hydrogen was retained at low temperature; EXAFS data of supported Pd by Moraweck *et al.* (*46*) and Davis *et al.*(*47*) show that the Pd–Pd lattice expands in Pd hydrides. With Pd particles as small as trimers, the distinction between adsorbed hydrogen and hydride hydrogen will vanish. Our reason for using a higher reduction and desorption temperature, 350°C, was that our previus TPR work had shown the necessity to ascertain complete desorption of strongly chemisorbed H from Pd particles (*26,27*). This is imperative for obtaining a reliable Pd–Pd bond distance characteristic of pure metallic clusters.

The present EXAFS results clearly demonstrate CO-induced Pd particle growth in the supercages of zeolite NaY. Future work must address two additional questions: (1) Is Pd particle growth irreversible upon removing adsorbed CO? (2) Does CO induce migration of isolated Pd atoms from sodalite cages to supercages?

ACKNOWLEDGMENTS

We thank Professor E. Stern for kindly donating his EXAFS package. A research grant from the National Science Foundation, Grant No. CTS11184 and financial support by a grant-in-aid of the Mobil Foundation Inc. are gratefully acknowledged. We also thank Dr. A. Bommannavar for his technical assistance during data collection and Professor K. R. Poeppelmeier for his kind permission to make use of some of his lab facilities.

REFERENCES

1. Cotton, F. A., and Wilkinson, G., "Advanced Inorganic Chemistry." Wiley, New York, 1980.
2. Cotton, F. A., and Wilkinson, G., *Advanced Inorganic Chemistry* 1988. p. 1024.
3. Cox, D. M., Reichmann, K. C., Trevor, D. J., and Kaldor, A., *J. Chem. Phys.* **88,** 111 (1988).
4. Sheu, L.L., Knözinger, H., and Sachtler, W. M. H., *Catal. Lett.* **2,** 129 (1989).
5. Sheu., L. L., Knözinger, H., and Sachtler, W. M. H., *J. Mol. Catal.* **57,** 61 (1989).
6. Sheu, L. L., Knözinger, H., and Sachtler, W. M. H., *J. Amer. Chem. Soc.* **111,** 8125 (1989).
7. Feltham, R. D., Elbaze, G., Ortega, R., Eck, C., and Dubrowski, J., *Inorg. Chem.* **24,** 1503 (1985).
8. Mednikov, E. G., Eremenko, N. K., Slovokhotov, Yu. L., Struchkov, Yu. T., and Gubin, S. P., *J. Organomet. Chem.* **258,** 247 (1983).
9. Mednikov, E. G., Eremenko, N. K., Gobin., S. P., Slovokhotov, Yu. L., and Struchkov, Yu. T., *J. Organomet. Chem.* **239,** 401 (1982).
10. Mednikov, E. G., Eremenko, N. K., Slovokhotov, Yu. L., and Struchkov, Yu. T., *J. Organomet. Chem.* **301,** C35 (1986).
11. Mednikov, E. G., Eremenko, N. K., Slovokhotov, Yu. L., and Struchkov, Yu. T., *J. Chem. Soc. Chem. Commun.*, 218 (1987).
12. Tsang, C. M., Augustine, S. M., Butt, J. B., and Sachtler, W. M. H., *Appl. Catal.* **46,** 45 (1989).
13. Dossi, C., Schaefer, J., and Sachtler, W. M. H., *J. Mol. Catal.* **52,** 193 (1989).
14. Sheu, L.-L., and Sachtler, W. M. H., unpublished.
15. Rao, L.-F., Fukuoka, A., Kosugi, N., Kuroda, H., and Ichikawa, M., personal communication, 1990.
16. Montovani, E., Palladino, N., and Zanobi, A., *J. Mol. Catal.* **3,** 28 (1977).
17. Gelin, P., Ben Taarit, Y., and Naccache, C., *J. Catal.* **59,** 357 (1979).
18. Rode, E. J., Davis, M. E., and Hanson, B. E., *J. Catal.* **96,** 574 (1985).
19. Gelin, P., Lefebvre, F., Elleuch, B., Naccache, C., and Ben Taarit, Y., *in* "Intrazeolite Chemistry" (G. D. Stuky and F. G. Dwyer, Eds.), ACS Symposium Series 218, p. 455. Amer. Chem. Soc., Washington, DC, 1983.
20. Wong, T., Zhang, Z., and Sachtler, W. M. H., *Catal. Lett.*, **4.** 365 and **5,** 331 (1990).
21. van't Blik, H. F. J., van Zon, J. B. A. D., Huizinga, T., Vis, J. C., Koningsberger, D. C., and Prins, R., *J. Amer. Chem. Soc.* **107,** 3139 (1985).
22. Bergeret, G., Gallezot, P., Gelin, P., Ben Taarit, Y., Lefebvre, F., Naccache, C., and Shanon, R. D., *J. Catal.* **104,** 279 (1987).
23. van't Blik, H. F. J., van Zon, J. B. A. D., Huizinga,

T., Vis, J. C., Koningsberger, D. C., and Prins, R., *J. Phys. Chem.* **87,** 2264 (1983).
24. Möller, K., and Bein, T., *J. Phys.*, C8-231 (1986).
25. Möller, K., and Bein, T., *J. Phys. Chem.* **93,** 6116 (1989).
26. Homeyer, S. T., and Sachtler, W. M. H., *J. Catal.* **117,** 91 (1989).
27. Homeyer, S. T., and Sachtler, W. M. H., *J. Catal.* **118,** 266 (1989).
28. Gurman, S. J., Binsted, H., and Ross, I., *J. Phys.* **17,** 143 (1984).
29. Gallezot, P., and Imelik, B., *Mol. Sieve Adv. Chem. Ser.* **121,** 66 (1973).
30. Bergeret, G., Tri, T. M., and Gallezot, P., *J. Phys. Chem.* **87,** 1160 (1983).
31. Bergeret, G., Gallezot, P., and Imelik, B., *J. Phys. Chem.* **85,** 411 (1981).
32. Purdum, H., Montano, P. A., Shenoy, G. K., and Morrison, T., *Phys. Rev. B* **25,** 4412 (1982).
33. Montano, P. A., and Shenoy, G. K., *Solid State Commun.* **35,** 53 (1980).
34. Apai, G., Hamilton, J. F., Stohr, J., and Thompson, A., *Phys. Rev. Lett.* **43,** 165 (1979).
35. Yokoyama, T., Kimoto, S., and Ohta, T., *Physica B* **158,** 255 (1989).
36. Fulde, P., Luther, A., and Watson, R. F., *Phys. Rev. B* **8,** 440 (1973).
37. van Santen, R. A., private communication.
38. Michalik, J., Heming, M., and Keven, L., *J. Phys. Chem.* **90,** 2132 (1986).
39. Narayana, Michalik, J., Contarini, S., and Kevan, L., *J. Phys. Chem.* **89,** 3895 (1985).
40. Homeyer, S. T., Karpinski, Z., and Sachtler, W. M. H., *J. Catal.* **123,** 60 (1990).
41. Zhang, Z., Wong, T., and Sachtler, W. M. H., in press.
42. Poel, E. K., Koolstra, R., Geus, J. W., and Ponec, V., *Stud. Surf. Sci. Catal.* **11,** 233 (1982).
43. Feltham, R. D., Elbaze, G., Ortega, R., Eck, C., and Dubrowski, *J. Inorg. Chem.* **24,** 1503 (1985).
44. Möller, K., and Bein, T., *J. Phys.* C8-231 (1986).
45. Möller, K., Koningsberger, D. C., and Bein, T., *J. Phys. Chem.* **93,** 6116 (1989).
46. Moraweck, B., Clugnet, G., and Renouprez, *J. Chim. Phys.* **83,** 265 (1983).
47. Davis, R. J., Landry, S. M., and Boudart, M., *Phys. Rev. B* **39,** 10580 (1989).